IEEE Access
Multidisciplinary | Rapid Review | Open Access Journal

Received January 22, 2019, accepted February 1, 2019, date of publication February 15, 2019, date of current version March 5, 2019.

Digital Object Identifier 10.1109/ACCESS.2019.2899624

A Competing Risk Model of Reliability Analysis for NAND-Based SSDs in Space Application

PENG LI[1,2], WEI DANG[1], TAICHUN QIN[3], ZEMING ZHANG[1], AND CONGMIN LV[1,2]

[1]Technology and Engineering Center for Space Utilization, Chinese Academy of Sciences, Beijing 100094, China
[2]University of Chinese Academy of Sciences, Beijing 100049, China
[3]Beijing Key Laboratory of Environment and Reliability Test Technology for Aerospace Mechanical and Electrical Products, Beijing Institute of Spacecraft Environment Engineering, Beijing 100094, China

Corresponding author: Congmin Lv (lvcongmin@csu.ac.cn)

This work was supported in part by the National Natural Science Foundation of China under Grant 61703391, and in part by the Technology and Engineering Center for Space Utilization under Grant CSU-QZKT201714.

ABSTRACT This paper develops a competing risk model to simultaneously analyze censored catastrophic failures and nonlinear degradation data of the NAND-based solid-state drives for space application. Two dominant failure modes are the hard failure of the controller due to single-event latch-up (SEL) and the soft failure of the NAND Flash manifesting as random write current degradation. As hard failure probability increases with radiation intensity and particle number, we establish the inverse power law-Weibull model for SEL cross section to model the accelerated censored data. The hard failure model is presented based on the invariance principle of total environmental particles' energy. On the other hand, soft degradation is described by the nonlinear Wiener-process-based accelerated degradation test model. Specifically, the temporal variability concerning the inherent variability of the degradation process over time and the unit-to-unit variability in degradation rates are both taken into account. Then, we derive the reliability functions and other quantities of interest under normal conditions with the assumption of independence of failure modes. Furthermore, to estimate the unknown parameters in the competing risk model, the transformed extreme value regression analysis other than the least square fitting method is adapted to issue the problem of data uncertainty of hard failures, whereas the maximum likelihood estimation method is developed for soft failures. Finally, a detailed simulation example is given to illustrate the procedure of the proposed reliability model with a sensitivity analysis.

INDEX TERMS Semiconductor device modeling, degradation, reliability engineering, space radiation, uncertainty.

I. INTRODUCTION

As the need for lower-cost, higher-density mass storage increases rapidly in space science and application field, solid-state drives (SSDs), especially commercial NAND-based SSDs, have been widely used by aerospace developers and space engineers due to their high-performance, low energy consumption, small size, and stable delivery period [1], [2]. Actually commercial off-the-shelf (COTS) NAND Flash was successfully used in Chinese Tiangong-1 as early as 2011. While the European space mission did not yet applied the Flash-based mass memory device until 2013 in Sentinel-2 [3]. It was reported that the number of SSDs shipped in 2016 alone exceeded 130 million units totaling around 50 exabytes of storage capacity [4]. For mission-critical SSD, their in-service failures, such as the loss of stored data can cause heavy economic losses or even severe casualties of human lives as a result of the harsh space environment. Compared with military SSDs, commercial SSDs can easily lower costs and offer technological innovations, contributing to their increasing popularity in the aerospace industry. However, COTS products are primarily designed for use in benign environments where equipment is easily accessed for repair or replacement, therefore their space application makes a matter of concern well beyond the consumer level of electronics [5]. As such, modeling and estimating their reliability and state of health under actual space environment accurately to demonstrate the feasibility and avoid catastrophic events is crucial and significant from both a cost-effective and a safety point of view.

The associate editor coordinating the review of this manuscript and approving it for publication was Nianqiang Li.

Since 2008, JEDEC commissioned a group of drives customers, SSD manufacturers, and NAND component manufactures to develop JESD218 and JESD219 standards for qualifying SSDs to clearly-specified endurance and retention specifications [6], [7]. More recent attention has focused on the reliability problem of SSD. Mielke *et al*. [8] reviewed SSD's reliability from the perspective of failure mechanisms and design mitigation techniques, with particular emphasis on the JEDEC qualification methods. Schroeder *et al*. [4] presented three large-scale reliability studies of NAND-based SSDs in production environments, subjected to real workloads and operating conditions by Facebook, Google and Microsoft. Compagnoni *et al*. [9] reviewed historical trends of NAND Flash technologies, explaining why the scaling of planar arrays below 1x nm is less favorable than vertical integration. Boyd *et al*. [10] conducted a life-cycle assessment of NAND Flash over five technology generations (150 nm, 120 nm, 90 nm, 65 nm, and 45 nm) to quantify environmental impacts occurring in Flash production and to view their trends over time. In general, SSDs experience multiple failure modes that compete against each other, and whichever occurs first can cause the failure.

Many people are theoretically devoted to the competing failures modeling and reliability evaluation considering multiple degradation failure processes, or degradation and catastrophic failure processes. Rafiee *et al*. [11] investigated reliability modeling for systems subject to dependent competing risks considering the impact from a new generalized mixed shock model, and the degradation rate and the hard failure threshold can simultaneously shift multiple times. Hao *et al*. [12] developed a reliability model for mutually dependent competing failure process based on stress-strength models and cumulative damage/shock model. Che *et al*. [13] introduced the Facilitation model to the shock process and developed a novel analytical competing reliability model with mutual dependence. Qiu and Cui *et al*. [14] evaluated systems competing reliability based on a dependent two-stage failure process involving with defect initialization and development stages. Hao and Yang [15] considered the impact of harmful shocks on temporal degradation performance, degradation rates as well as hard failure threshold levels and developed a system reliability model subject to dependent competing failure processes. Haghighi and Bae [16] proposed a modeling approach to simultaneously analyze linear degradation and traumatic failures with competing risks in a step-stress accelerated degradation test based on cumulative exposure model. Fan *et al.* [17] developed a competing failure process model with degradation-shock dependence for an aviation spool valve. A semi-analytical framework is developed in modeling dependent competing failure processes based on stochastic hybrid systems [18]. In [19], a sequential Bayesian approach is developed for remaining useful life prediction of dependent competing failure processes. As reviewed above, the majority of these studies focuses on dependent shock and degradation process in the competing model, and there are fewer models considering space radiation and degradation competing failures. Additionally, research and literature on commercial SSD reliability under the safety-critical environment are not as established as in the industrial circles.

In most cases, the expense of radiation test is pretty high, and the radiation facility is source-constrained. We might only obtain censored data as the test duration allowed is fixed and limited. Besides, there exist great uncertainties with small testing samples, usually resulting in insufficient or missing data. Thus, in order to take full use of the censored data under different situations and evaluate the reliability more precisely, a regression analysis method should be proposed over the regular MLE method for catastrophic failures or hard failures. On the other hand, since lifetime data are often hard to obtain, degradation data can be used as an alternative resource for reliability analysis. Generally, the degradation of a product's physical property is related to its reliability, such as the growth of fatigue cracks and light intensity degradation, so a degradation failure, also called soft failure, is usually defined in terms of a performance characteristic exceeding a specified threshold. For instance, a battery that supplies electrical power by chemical reaction weakens during usage [20]. Unfortunately, reliability estimation can still be difficult to perform for it is nearly impossible to obtain a sufficient amount degradation data within acceptable testing time by testing them under normal operating environments [21]. Take SSD as an example, the manufacturers usually state in the data sheets that their flash memory has data retention of 5000 Program/Erase (P/E) cycles. Since, for obvious reasons of time to market, it is not feasible to test the flash memory for 20 years. As a result, to understand the reliability characteristics and lifetime under field conditions, the Wiener-process-based accelerated degradation test (ADT) models with higher stress levels are proposed to solve the reliability estimation problem. Actually, there extensively exists nonlinearity in practice, and it plays a vital role in the degradation processes. Nevertheless, the conventional ADT model cannot trace the dynamics of such a degradation process. It is more likely that degradation may accelerate at a later stage of life [22]. Therefore, the nonlinear Wiener-process-based ADT modeling and prognostics issues deserve to be addressed for degradation failures or soft failures [23].

All the above introductory remarks lead to the conclusion that the hard failure model, the soft failure model uncertainty and the regression analysis method for censored data are all essential features to be taken into consideration. However, until very recently, our knowledge about SSD reliability was derived from controlled experiments in lab environments under synthetic workloads, often using methods for accelerated testing that put the drive through many cycles to synthetically speed up wear-out, based on JEDEC standards [6], [7]. Furthermore, few works have been witnessed on the competing risk model of reliability analysis for NAND-based SSDs in space application. This paper aims to address this problem, and allow the analyst to develop a competing risk model considering censored failures and nonlinear Wiener-process-based ADT model with temporal variability and unit-to-unit

variability, and predict the reliability of SSDs using both hard and soft failures. Additionally, the Weibull regression analysis method for censored data and the MLE method for degradation data are derived to estimate the model parameters.

The remainder of the paper is organized as follows. Section II describes the basic information of SSD, conducts failure and stress analysis. Model assumption, reliability modeling and analysis for an individual hard and soft failure mode and competing risk model are respectively developed in Section III. In Section IV, the parameter estimation for the competing risk model, including Weibull regression analysis method and MLE method are studied respectively. Section V presents the SSD numerical example to estimate reliability and remaining useful life (RUL), and sensitivity analysis of model parameters is also discussed. Section VI summarizes the article and makes concluding remarks.

II. FAILURE MECHANISMS OF THE SSD

A. SSD DESCRIPTION

As shown in Figure 1, the NAND-based SSD is responsible for transferring data and communicates with the host by Serial ATA (SATA) III interface, and its main parts are the controller, the SDRAM, the NAND Flash, and the power supply protection circuit. The controller is a microprocessor with SSD-specific support circuits, typically using an external DRAM for its working memory and running firmware, and it allocates data to NAND Flash components after translating the logical address into the physical address. NAND Flash components for storing data take up the majority of the board space in an SSD, and each component may contain multiple NAND integrated circuits (ICs). The protection circuit converts the input to a steady low-voltage supply for other components. Data and power are respectively connected to the controller and power supply through the SATA III interface.

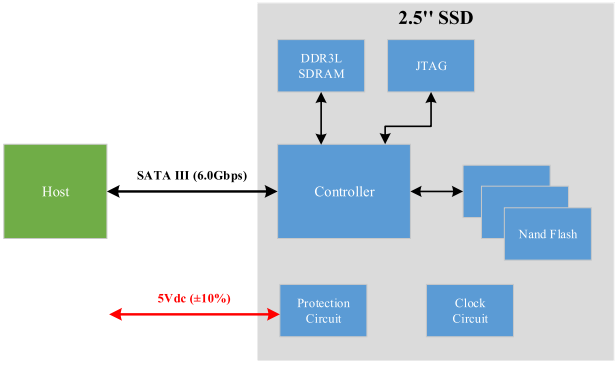

FIGURE 1. Function and schematic diagram of SSD.

There are three main performance indexes of SSD: operating current, read-write speed, and bad blocks. However, as wear leveling techniques are extensively adopted to reduce wear on storage cells by dispersing write operations throughout the available storage area, bad blocks numbers remain nearly unchanged under limited operating time. According to historical test results and previous research [24], only the operating current and read-write speed are monitored to detect the state of the controller, while random write current is taken as the health indicator of NAND Flash.

B. FAILURE MECHANISM ANALYSIS

Though the spacecraft takes thermal control, anti-static, and radiation protection measures, SSDs would still be exposed to extremely harsh mission environment. In this study, we leave out the stage of transportation and launch, and focus on the on-orbit life cycle. As shown in Table 1, on-orbit SSD should experience space environment stresses, operating stresses and platform stresses.

TABLE 1. Space environment effect analysis for on-orbit SSD.

Mission environment		Effect
Space environment stresses	Ionizing radiation	TID & SEE
	High temperature	Tunnel oxide degradation
	Vacuum	Outgas effect
	Space light radiation	Material aging
	Plasma	Charging and discharging effect
Operating stresses	Voltage	Dielectric breakdown
	P/E cycles	Wearout
Platform stresses	Micro-vibration & shock	Fatigue crack

For platform environment, micro-meteors and orbital debris induced platform micro-vibration and shock may cause fretting wear and fatigue for tiny relative motion of connector's contact area, and then result in coat peeling and contact point fracture, etc. A common effect of this latent defects is to cause adjacent interconnects to short together because the dielectric separating them breaks down. However, this issue can be avoided by platform design of vibration isolation. Besides, screening test before delivery can effectively prevent this early process defects. For operation environment, even though voltage-related dielectric breakdown, whether intrinsic or defect related, can lead to the failure of SSD, and actually the probability of dielectric breakdown is exponentially dependent on the applied voltage, the steady input voltage can be guaranteed by the spacecraft system. Frequent P/E cycles weaken the chemical bond for the insulating floating gate (FG), and worsen insulating layer effect, making electrons easy to escape. Consequent flash degradation can increase the incidence of retention errors, read disturb errors and write errors. But the total P/E cycles are absolutely enough compared with the amount of mission data. For space environment, weightlessness and electromagnetic interference caused by space gravitational field have little influence on SSD; SSD can be directly affected by ionizing radiation in the form of total ionizing dose (TID) and single event effects (SEE); high temperature can gradually worsen the NAND Flash performance; vacuum outgas results in molecule contamination, such as the increase of contact resistance. Nevertheless, this effect can be negligible as ground thermal vacuum test is compulsory at least in system level and the performance of SSD should be assessed; space light radiation may merely cause material aging and coating damage; plasma-induced charge and discharge commonly affect the

surface material and coating of the spacecraft, and the effect on SSD can be ignored due to enclosure protection; To sum up, ionizing radiation and high temperature are crucial and deserve further analysis.

The ionizing radiation effects could range from minor degradation to complete device failure and therefore threaten the overall mission. In most cases, no permanent damage is done, but the affected circuit will temporarily mis-operate. This soft error caused by ionizing radiation is a transient error in an IC. TID tends to become less significant presumably because of very thin high k oxides and general feature shrinking. An SEE is a disturbance to the normal operation of a circuit caused by the passage of a single ion through or near a sensitive node in a circuit, and it can be either destructive or non-destructive. SEE mechanisms are becoming less severe in terms of survivability of the device but more widespread due to the physical (3-D) stacking of the bare chips. Heavy ion induced SEE such as single event transient, single event upset, single event functional interrupt, or single event latchup (SEL) are of major concern [25]. NAND soft errors are confirmed to be minimal compared to the controller because NAND has a low soft error rate that can be handled by the strong error-correction code. Through design mitigations, it has been experimentally verified that radiation-induced soft errors can be removed by reset and/or power cycling without any loss of data. SEL is among the most important reliability concerns for electronics deployed in space systems. Despite a lower bias voltage, latchup is still an issue. The current would show an abrupt jump and then continue to increase. The radiation of high-energy particles causes the plasma track, triggering the charge to flow within the track, and then catastrophic large current might heat the chip all the way to fail [26]. The chip's parasitic devices or weak links are activated, resulting in permanent changes in the chip's characteristics or functions, and the SSD cannot recover even after a reboot. Thus, SEL often causes more complex failure modes of the controller. For the flip chip of NAND SSD, the laser test is an alternative way to replace the ionizing radiation test. It is financially preferable to choose the pulse laser experiment in National Space Science Center than Heavy Ion Research Facility in Lanzhou (HIRFL) and HI-13 tandem accelerator of China Institute of Atomic Energy.

Some wear mechanisms may play a role in characterizing the NAND Flash lifetime. A flash memory basically works on a floating gate (FG) transistor. The programming operation injects electrons in the FG, while the erase operation does the opposite operation. However the FG is subject to wear and damage. Due to the phenomenon of Fowler-Nordheim (FN) tunneling, electrons in memory cells write in or read out data in the NAND flash memory by passing through tunnel oxide repeatedly. This process contributes to the gradual degradation of the tunnel oxide. As the environment temperature rises, the thermal motion energy of electrons increases, accelerating the destruction of tunnel oxide in tunneling. Besides, for multi-level cell (MLC) Flash, every cell store a 2-bit data, this is to say that the electrical level is divided into 4 levels [27]. Once Flash electrical level drifts, raw bit errors occur, whereas the distribution of electrical level depends on temperature. The raw bit error rate (RBER) of NAND Flash increases with increasing temperature. As a result, high temperature can gradually worsen the write/read performance of NAND Flash, leading to the entire SSD to fail.

In summary, based on the structure, function, and space environment effect analysis, it suggests radiation test and thermal test are significant and effective to investigate the reliable utilization of commercial SSDs in space application.

III. MODEL DESCRIPTION

A. MODEL ASSUMPTION

According to the failure mechanism classification of overstress and cumulative-stress failure, NAND-based SSDs presents two dominant failure modes: the hard failure of the controller due to single event latch-up (SEL), and the soft failure of the NAND Flash manifesting as random write current degradation. The competing failure mode is proposed to describe the failure process of an SSD under the hypotheses that (1) the two failure modes are independent of each other, as each failure mode is caused by a different stress and the physical mechanisms that influence the evolution of each failure mode are quite unrelated without regard to manufacturing defects in early age, and radiation-induced soft errors, and (2) the control unit and NAND Flash are connected in series and any of the following conditions make the SSD fail: a) the magnitude of any radiation exceeds the threshold value L, or b) the current drift of the NAND Flash is beyond the degradation failure threshold H [28], [29].

B. RELIABILITY MODELING OF THE HARD FAILURE

The exposure to space radiation may cause the SSD suddenly fails at a certain time when the linear energy transfer (LET) exceeds the threshold value [30]. Failure data can be used to estimate reliability and lifetime, and hard failure mode is caused by SEL. According to the previous engineering experience, its reliability and cumulative distribution function (cdf) can be properly described by Weibull distribution with shape parameter m and scale parameter $\eta(r)$ at time t and LET level r:

$$R_s(t) = \exp\left[-\left(t/\eta(r)\right)^{\beta}\right] \tag{1}$$

$$F_s(t) = 1 - \exp\left[-\left(t/\eta(r)\right)^{\beta}\right] \tag{2}$$

Ground radiation simulation test is performed with heavy ions having different LETs or various pulse laser energy. Then SEL cross section σ_{SEL} under every testing LET value can be calculated by frequency ratio or area ratio. Furthermore, the SEL cross section curve covering the whole practical LET environment data on certain orbit can also be plotted [31]. Actually classical reliability models can be mapped from the time domain to the fluence domain. For selected ranges of LETs, we usually use an upper bound of particle flux (number of particles/cm^2 • s^{-1}) to determine if

the item can meet the mission's reliability requirements. The life characteristic is represented as:

$$\eta(r) = \frac{r}{\sigma_{SEL}(r)\int_0^{r_{\max}} flux(r)\,dr} \tag{3}$$

Hence, mapping from the time domain to the fluence domain (per LET) is straight-forward. For a given LET, SEL are independent, and σ_{SEL} is constant, the mean fluence to failure (MFTF) is:

$$MFTF = {}^{1}/_{\sigma_{SEE}} \tag{4}$$

The SSDs actually experience a low radiation intensity either continuously or intermittently in the space environment. As the total particles number with certain energy is equal under the accelerated and usual situation. The dose or rate are raised to a high level in the laboratory test to compress test length. In the absence of information regarding the underlying process of space radiation, the SEL cross section is assumed to follow a power function:

$$\sigma_{SEL} = e^{a} r^{b} \tag{5}$$

The increase of intensity might have effects on the characteristic life, and then the SEL acceleration factor is

$$AF = \frac{MFTF(r_0)}{MFTF(r_i)} = \frac{\sigma_{SEL}(r_i)}{\sigma_{SEL}(r_0)} = \left(\frac{r_i}{r_0}\right)^{b} \tag{6}$$

Thus, increasing r: 1) shortens lifetime if $b > 0$; 2) makes no difference on lifetime if $b = 0$; 3) prolongs lifetime if $b < 0$. The paper deal with the case when $b > 0$, to shorten test length, and m is independent of stress level r. Apparently, the relationship between $\eta(r)$ and r is an inverse power law model through a logarithmic transformation:

$$\ln \sigma_{SEL}(r) = a + b \ln r \tag{7}$$

Due to the limited testing time, constrained facility and test uncertainty, the results data are usually censored. The censored times are specified. Moreover, the specified r_{max} is determined by using engineering judgment, experience, similar data, and/or preliminary tests, and it should be as high as possible to shorten test length and generate more failures. However, it should not result in new failure modes different from those at r_0.

In order to make the most of the censored data under different LET levels, the transformed extreme value regression analysis method is established. Let $y = \ln t$, thus y follows extreme value distribution.

$$F_s(y) = 1 - \exp\left[-\exp\left(\frac{y - \mu(r)}{\sigma}\right)\right] \tag{8}$$

where $\mu(r)$ and σ are location and scale parameters

$$\begin{cases} \mu(r) = \ln \sigma_{SEL}(r) \\ \sigma = 1/m \end{cases} \tag{9}$$

A linear relationship between $\mu(r)$ and r is given:

$$\mu(r) = a + b \ln r \tag{10}$$

Then y is ex pressed as

$$y = a + b \ln r + \varepsilon \tag{11}$$

where $\varepsilon \sim$ EV(0, σ), and a, b, σ are parameters to be estimated.

C. RELIABILITY MODELING OF THE SOFT FAILURE

The random write current would continuously degrade under high-temperature aging until the NAND Flash exhibits an unsatisfactory performance. To capture the dynamics of the degradation process, and lead to a better understanding of the nature of the failure event, we use a stochastic process with a nonlinear path to characterize the random write current degradation. Moreover, as each item possibly experiences different sources of variations during its operation, we incorporate item-to-item variability with the nonlinear Wiener-process-based ADT model [32].

Let $X(t)$ denote the degradation at time t under stress level S, which is driven by a standard Brownian motion $B(t)$ with a constant diffusion coefficient σ_B and a nonlinear drift of $\lambda(t;\psi) = ce^{-d/S}t^{\alpha}$. By ignoring the measurement error, the stochastic process becomes:

$$X(t) = X(0) + \lambda(t;\psi) + \sigma_B B(t) \tag{12}$$

where ψ is the parameter vector, $X(0)$ is the initial degradation, c is a random effect reflecting unit-unit variation, and d is a fixed effect suitable for all products.

The lifetime T_w is regarded as the first hitting time that the long-term drift reaches a pre-set failure threshold H, and the case $X(0) = 0$ is considered below without loss of generality [33].

$$T_w = \inf\{t : X(t) \geq H\} \tag{13}$$

The probability density function (pdf) of the lifetime can be formulated as:

$$f_w(t;c) = \frac{H - ce^{-d/S}t^{\alpha}(1-\alpha)}{\sigma_B^2\sqrt{2\pi t^3}} \exp\left[-\frac{\left(H - ce^{-d/S}t^{\alpha}\right)^2}{2\sigma_B^2 t}\right] \tag{14}$$

For simplicity, random effect c is assumed to follow a normal distribution with mean μ_c and variance σ_c^2. According to the law of total probability, the pdf of the lifetime for a nonlinear Wiener process with random effects is given by:

$$\begin{aligned} f_w(t) &= \int_{-\infty}^{+\infty} f_w(t;c) f(c) dc E_c\left[f_w(t;c)\right] \\ &= \frac{1}{\sqrt{2\pi t^3\left(e^{-2d/S}t^{2\alpha-1}\sigma_c^2 + \sigma_B^2\right)}} \\ &\quad \times \left[H - e^{-d/S}t^{\alpha}(1-\alpha)\frac{e^{-d/S}t^{\alpha-1}\sigma_c^2 H + \mu_c\sigma_B^2}{e^{-2d/S}t^{2\alpha-1}\sigma_c^2 + \sigma_B^2}\right] \\ &\quad \times \exp\left[-\frac{\left(H - e^{-d/S}t^{\alpha}\mu_c\right)^2}{2\left(e^{-2d/S}t^{2\alpha}\sigma_c^2 + \sigma_B^2 t\right)}\right] \end{aligned} \tag{15}$$

Since the analytical form of $R_w(t)$ can be difficult to obtain, a numerical integration method can be utilized:

$$R_w(t) = 1 - \int_0^t f_w(t)\,dt \tag{16}$$

D. COMPETING RISK MODEL

As different independent failure mechanisms have different development rate, the competition process means the system failure time will be determined by the mechanism which develops to failure first. Under the assumption of independent competing rule, the reliability relies on the minimum life among the multiple random lives:

$$\begin{aligned} R_c(t) &= P\{T_c > t\} = P\{\min\{T_s; T_w\} > t\} \\ &= P\{T_s > t\}\,P\{T_w > t\} \\ &= R_s(t)\,R_w(t) \end{aligned} \tag{17}$$

The cdf under the competing risk model is given by:

$$F_c(t) = 1 - (1 - F_s(t))\,(1 - F_w(t)) \tag{18}$$

In many cases, we should figure out which failure mode is more likely to cause the final failure in a specific duration. The pdf that the SSD fails on a soft failure in the presence of both failure modes is stated as follows

$$\begin{aligned} f_{c,w}(t) &= f_w(t)\,R_s(t) \\ &= \frac{1}{\sqrt{2\pi t^3\left(e^{-2d/S}t^{2\alpha-1}\sigma_c^2 + \sigma_B^2\right)}} \\ &\quad\times\left[H - e^{-d/S}t^{\alpha}(1-\alpha)\frac{e^{-d/S}t^{\alpha-1}\sigma_c^2 H + \mu_c\sigma_B^2}{e^{-2d/S}t^{2\alpha-1}\sigma_c^2 + \sigma_B^2}\right] \\ &\quad\times\exp\left[-\frac{\left(H - e^{-d/S}t^{\alpha}\mu_c\right)^2}{2\left(e^{-2d/S}t^{2\alpha}\sigma_c^2 + \sigma_B^2 t\right)}\right] \\ &\quad\times\exp\left[-\left(t/\eta(r)\right)^{\beta}\right] \end{aligned} \tag{19}$$

By the integral operation, the probability function $F_{c,w}(t)$ caused by each failure mode during the whole life can be calculated when the mission time t tend to be infinite. Similarly, the pdf $f_{c,s}(t)$ and cdf $F_{c,s}(t)$ of the hard failure can also be formulated. For competing failures, it turns out to be:

$$\begin{aligned} f_c(t) &= f_{c,w}(t) + f_{c,s}(t) \\ F_c(t) &= F_{c,w}(t) + F_{c,s}(t) \end{aligned} \tag{20}$$

The mean time to failure (MTTF) for the competing risk model can be derived through:

$$MTTF = \int_0^{\infty} R_c(t)\,dt \tag{21}$$

Besides, RUL, known as the length between the current inspection time and the end of the allowed useful life, is crucial to estimate at the design or testing stages so as to recommend future maintenance and schedule making for replacement. It can be written as $L_t = \{L : T_c - t\,|T_c > t\}$. As long as continuous monitoring data is available, the individually estimated RUL is beneficial to make dynamic management. Then the pdf of RUL is expressed as:

$$f_{L_t}(L) = f_c(t + L)\big/R_c(t) \tag{22}$$

IV. PARAMETER ESTIMATION

Since the two failure modes are independent, and parameters are quite unrelated, in this study, the parameters of the competing risk model can be estimated separately for each failure mode. Next, the Weibull regression analysis method for censored failure data and the MLE method for degradation data are illustrated respectively.

A. ESTIMATE OF HARD FAILURE MODEL PARAMETER

There are n_i samples tested under different LET levels r_i, and q_i of them fail at the censored time y_i^*. The time-censored failure data $y_{i1} \le y_{i2} \le \ldots \le y_{iq_i}$ can be regarded as a value of the first q_i order statistics $Y_{i1} \le Y_{i2} \le \ldots \le Y_{iq_i}$ from an extreme value distribution with size n_i. Then $y_{i(q_i+1)} = y_i^*$ is seen as a value of the q_ith interval statistics from the same samples.

$$y_{ik} = a + b\ln r_{ik} + \varepsilon_{ik} \tag{23}$$

$$Q = \sum_{i=1}^{m}\sum_{k,l=1}^{q_i+1}\left[\begin{array}{l}(y_{ik} - a - b\ln r_i - \sigma u_{ik}) \\ \times v^{ikl}\,(y_{il} - a - b\ln r_i - \sigma u_{il})\end{array}\right] \tag{24}$$

where $\left[v^{ikl}\right]_{(q_i+1)\times(q_i+1)} = \left[v^{ikl}\right]^{-1}_{(q_i+1)\times(q_i+1)}$, and $u_{ik}(k = 1, 2, \cdots, q_i)$ is the mean of the kth order statistics and $v_{ik}(k = 1, 2, \cdots, q_i)$ is the covariance of the kth and the lth order statistics of the standard extreme value distribution with size n_i, while $u_{i(qi+1)}$ is the mean of the q_i+1th order statistics and $v_{ik(qi+1)} = v_{i(qi+1)k}(k = 1, 2, \cdots, q_i + 1)$ is the covariance of the standard extreme value distribution with size $n_i + 1$. All these parameters can be caculated or obtained in [34].

Let the derivatives of Q with respect to a, b and σ to zero, and the best unbiased integral estimation of the regression coefficients and the standard deviation can be obtained by logarithmic regression analysis of censored data:

$$\hat{a} = \bar{y} - \hat{b}\ln\bar{r} - \hat{\sigma}\bar{u} \tag{25}$$

$$\hat{b} = \frac{L_{22}L_{1y} - L_{12}L_{2y}}{L_{11}L_{22} - L_{12}^2} \tag{26}$$

$$\hat{\sigma} = \frac{L_{11}L_{2y} - L_{12}L_{1y}}{L_{11}L_{22} - L_{12}^2} \tag{27}$$

where

$$\bar{y} = \frac{1}{n^*}\sum_{i=1}^{m}\sum_{k,l=1}^{q_i+1} v^{ikl}y_{ik},\ \bar{u} = \frac{1}{n^*}\sum_{i=1}^{m}\sum_{k,l=1}^{q_i+1} v^{ikl}u_{ik}$$

$$\ln\bar{r} = \frac{1}{n^*}\sum_{i=1}^{m}\sum_{k,l=1}^{q_i+1} v^{ikl}\ln r_i,\quad n^* = \sum_{i=1}^{m}\sum_{k,l=1}^{q_i+1} v^{ikl}$$

$$L_{1y} = \sum_{i=1}^{m}\sum_{k,l=1}^{q_i+1} v^{ikl}\left(\ln r_i - \ln\bar{r}\right)\left(y_{ik} - \bar{y}\right)$$

$$L_{2y} = \sum_{i=1}^{m} \sum_{k,l=1}^{q_i+1} \upsilon^{ikl} (u_{ik} - \bar{u}) (y_{il} - \bar{y})$$
$$L_{11} = \sum_{i=1}^{m} \sum_{k,l=1}^{q_i+1} \upsilon^{ikl} (\ln r_i - \ln \bar{r})^2$$
$$L_{12} = \sum_{i=1}^{m} \sum_{k,l=1}^{q_i+1} \upsilon^{ikl} (\ln r_i - \ln \bar{r}) (u_{ik} - \bar{u})$$
$$L_{22} = \sum_{i=1}^{m} \sum_{k,l=1}^{q_i+1} \upsilon^{ikl} (u_{ik} - \bar{u}) (u_{il} - \bar{u})$$

The one-side upper and lower limits with confidence coefficient γ for position parameter $\mu(r)$ and scale parameter σ under certain LET r are given respectively:

$$\begin{cases} \mu_{up}(r) = \hat{a} + \hat{b}r + \dfrac{\hat{\sigma} u_\gamma}{1 - u_\gamma^2 c_{33}} \left[u_\gamma (c_{13} + c_{23} r) + \sqrt{\omega} \right] \\ \mu_{low}(r) = \hat{a} + \hat{b}r + \dfrac{\hat{\sigma} u_\gamma}{1 - u_\gamma^2 c_{33}} \left[u_\gamma (c_{13} + c_{23} r) - \sqrt{\omega} \right] \end{cases} \tag{28}$$

$$\begin{cases} \sigma_{up} = \dfrac{\hat{\sigma}}{1 - u_\gamma \sqrt{c_{33}}} \\ \sigma_{low} = \dfrac{\hat{\sigma}}{1 + u_\gamma \sqrt{c_{33}}} \end{cases} \tag{29}$$

where u_γ is the γ quantile for a standard normal distribution,

$$\omega = u_\gamma^2 (c_{13} + c_{23} r)^2 + \left(1 - c_{33} u_\gamma^2\right) \left(c_{11} + 2c_{12} r + c_{22} r^2\right) \left(c_{j_1 j_2}\right)_{3\times 3}$$
$$= \begin{bmatrix} \sum_{i=1}^{m} \sum_{k,l=1}^{q_i+1} \upsilon^{ikl} & \sum_{i=1}^{m} \sum_{k,l=1}^{q_i+1} \upsilon^{ikl} r_i & \sum_{i=1}^{m} \sum_{k,l=1}^{q_i+1} \upsilon^{ikl} u_{ik} \\ \sum_{i=1}^{m} \sum_{k,l=1}^{q_i+1} \upsilon^{ikl} r_i & \sum_{i=1}^{m} \sum_{k,l=1}^{q_i+1} \upsilon^{ikl} r_i^2 & \sum_{i=1}^{m} \sum_{k,l=1}^{q_i+1} \upsilon^{ikl} r_i u_{ik} \\ \sum_{i=1}^{m} \sum_{k,l=1}^{q_i+1} \upsilon^{ikl} u_{ik} & \sum_{i=1}^{m} \sum_{k,l=1}^{q_i+1} \upsilon^{ikl} r_i u_{ik} & \sum_{i=1}^{m} \sum_{k,l=1}^{q_i+1} \upsilon^{ikl} u_{ik} u_{il} \end{bmatrix}^{-1}$$

The confidence intervals for position parameter $\mu(r)$ and scale parameter σ with confidence coefficient 2γ-1 are $[\mu_{low}(r), \mu_{up}(r)]$ and $[\sigma_{low}, \sigma_{up}]$.

$$\begin{cases} P\left\{\mu_{low}(r) \le \mu(r) \le \mu_{up}(r)\right\} = 2\gamma - 1 \\ P\left\{\sigma_{low} \le \sigma \le \sigma_{up}\right\} = 2\gamma - 1 \end{cases} \tag{30}$$

After obtaining $\hat{a}, \hat{b}$ and $\hat{\sigma}$, we can acquire the estimation of Weibull parameters $\hat{m}$ and $\hat{\eta}(r)$. Furthermore, for these several sets of censored data under different accelerated stresses, the parameters of inverse power law - Weibull model for SEL are estimated

$$\begin{cases} \sigma_{SEL}(r) = \exp \hat{\mu}(r) \\ \hat{m} = 1/\hat{\sigma} \end{cases} \tag{31}$$

B. ESTIMATE OF SOFT FAILURE MODEL PARAMETER

Suppose thermal test stress levels are $\boldsymbol{S} = \{S_1, S_2, \ldots, S_K\}$, and under the kth temperature level S_k, J measurements for the ith product are observed at times $t_{i,j,k}$, where $i = 1, 2, \ldots, N; k = 1, 2, \ldots, K; j = 1, 2, \ldots, J$. The corresponding degradation measurements are denoted by $x_{i,j,k}$. Denote the observation times vectors $\boldsymbol{t_{i,k}} = (t_{i,1,k}, t_{i,2,k}, \ldots t_{i,J,k})^{\mathrm{T}}$, $\boldsymbol{T_{i,k}} = \left(t_{i,1,k}^{\alpha}, t_{i,2,k}^{\alpha}, \cdots, t_{i,J,k}^{\alpha}\right)^T$, and the measurements vectors $\boldsymbol{x_{i,k}} = (x_{i,1,k}, x_{i,2,k}, \ldots, x_{i,J,k})^{\mathrm{T}}$. $\boldsymbol{x_{i,k}}$ follows a multivariate normal distribution with mean and variance based on the s-independent assumption of Brownian motion [35].

$$\mu_{x_{i,k}} = \mu_c e^{-d/S_k} T_{i,k} \tag{32}$$
$$\Sigma_{i,k} = e^{-2d/S_k} \sigma_c^2 T_{i,k} T_{i,k}^T + \Omega_{i,k} \tag{33}$$

where

$$\Omega_{i,k} = \sigma_B^2 Q_{i,k}, \quad Q_{i,k} = \begin{bmatrix} t_{i,1} & t_{i,1} & \cdots & t_{i,1} \\ t_{i,1} & t_{i,2} & \cdots & t_{i,2} \\ \vdots & \vdots & \ddots & \vdots \\ t_{i,1} & t_{i,2} & \cdots & t_{i,J_{i,k}} \end{bmatrix}$$

Therefore, the likelihood function based on the degradation model over parameter set $\theta = \left(\mu_c, \sigma_c^2, \sigma_B^2, d, \alpha\right)^T$ can be derived by

$$f_{x_{i,k}}(x|\theta, S) = \prod_{i}^{N} \prod_{k}^{K} \left\{ \frac{1}{(2\pi)^{J_{i,k}/2} \sqrt{|\Sigma_{i,k}|}} \times \exp\left[-\frac{1}{2} \left(x - \mu_{x_{i,k}}\right)^T \Sigma_{i,k}^{-1} \left(x - \mu_{x_{i,k}}\right) \right] \right\} \tag{34}$$

Due to the s-independence assumption of the degradation measurements of different items, the log-likelihood function can be written as

$$\ln L(\theta; x, S) = -\frac{JKN \ln(2\pi)}{2} - \frac{1}{2} \sum_{i=1}^{N} \sum_{k=1}^{K} \ln \left|\Sigma_{i,k}\right| - \frac{1}{2} \sum_{i=1}^{N} \sum_{k=1}^{K} \left(x_{i,k} - \mu_c e^{-d/S_k} T_{i,k}\right)^T \times \Sigma_{i,k}^{-1} \left(x_{i,k} - \mu_c e^{-d/S_k} T_{i,k}\right) \tag{35}$$

where

$$\left|\Sigma_{i,k}\right| = \left|\Omega_{i,k}\right| \left(1 + \sigma_c^2 e^{-d/S_k} T_{i,k}^T \Omega_{i,k}^{-1} T_{i,k}\right),$$
$$\Sigma_{i,k}^{-1} = \Omega_{i,k}^{-1} - \frac{\sigma_c^2 e^{-d/S_k}}{1 + \sigma_c^2 e^{-d/S_k} T_{i,k}^T \Omega_{i,k}^{-1} T_{i,k}} \Omega_{i,k}^{-1} T_{i,k} T_{i,k}^T \Omega_{i,k}^{-1}$$

As all items are measured at the same time, the number of measurements of each item is the same. Take the first partial derivatives of the log-likelihood function with respect to μ_c, σ_c^2 (36) and (37), as shown at the top of the next page.

For specific values of d, α, σ_B^2, though it is difficult to obtain the exact value by (32), we can easily obtain the

$$\frac{\partial \ln L(\theta; x, S)}{\partial \mu_c} = \frac{\sum_{i=1}^{N}\sum_{k=1}^{K} T^T \Omega^{-1} x_{i,k} - N\sum_{k=1}^{K} \mu_c e^{-d/S_k} T^T \Omega^{-1} T}{1 + \sum_{k=1}^{K} \sigma_c^2 e^{-2d/S_k} T^T \Omega^{-1} T} \tag{36}$$

$$\begin{aligned}\frac{\partial \ln L(\theta; x, S)}{\partial \sigma_c} &= -\frac{\sum_{k=1}^{K} \sigma_c N e^{-2d/S_k} T^T \Omega^{-1} T}{1 + \sum_{k=1}^{K} \sigma_c^2 e^{-2d/S_k} T^T \Omega^{-1} T} \\ &\quad + \frac{\sum_{i=1}^{N}\sum_{k=1}^{K} \sigma_c \left(x_{i,k} - \mu_c e^{-d/S_k} T\right)^T \Omega^{-1} T \Omega^{-1} T^T \left(x_{i,k} - \mu_c e^{-d/S_k} T\right)}{\left(1 + \sum_{k=1}^{K} \sigma_c^2 e^{-2d/S_k} T^T \Omega^{-1} T\right)^2}\end{aligned} \tag{37}$$

restricted MLE results of μ_c, σ_c^2 by setting their derivatives equal to zero:

$$\hat{\mu}_c = \frac{\sum_{i=1}^{N}\sum_{k=1}^{K} T^T \Omega^{-1} x_{i,k}}{N\sum_{k=1}^{K} e^{-d/S_k} T^T \Omega^{-1} T} \tag{38}$$

$$\hat{\sigma}_c^2 = \sum_{k=1}^{K} \left\{ \begin{array}{l} \frac{1}{N\left(e^{-2d/S_k} T^T \Omega^{-1} T\right)^2} \\ \times \sum_{i=1}^{N} \left[\begin{array}{l} \left(x_{i,k} - \mu_c e^{-d/S_k} T\right)^T \\ \times \Omega^{-1} T T^T \Omega^{-1} \left(x_{i,k} - \mu_c e^{-d/S_k} T\right) \end{array} \right] \\ - \frac{1}{e^{-2d/S_k} T^T \Omega^{-1} T} \end{array} \right\} \tag{39}$$

To estimate other parameters, the log-likelihood function with restricted MLE $\hat{\mu}_c$, $\hat{\sigma}_c^2$ can be expressed as

$$\begin{aligned}&\ln L\left(\sigma_B^2, d, \alpha; X, S, \hat{\mu}_c, \hat{\sigma}_c^2\right) \\ &= -\frac{JKN \ln(2\pi)}{2} - \frac{1}{2} N \sum_{k=1}^{K} \ln |\Sigma_k| \\ &\quad - \frac{1}{2}\sum_{i=1}^{N}\sum_{k=1}^{K} \left(x_{i,k} - \hat{\mu}_c e^{-d/S_k} T\right)^T \Sigma^{-1} \left(x_{i,k} - \hat{\mu}_c e^{-d/S_k} T\right)\end{aligned} \tag{40}$$

Then the MLE of d, α, σ_B^2 can be acquired by maximizing the log-likelihood function through a multi-dimensional search, and the final MLE for μ_c, σ_c^2 can be obtained by substituting $\hat{\sigma}_B^2$, $\hat{d}$, $\hat{\alpha}$.

V. NUMERICAL RESULTS

The testing 128GB 2.5-inch client-level SSD applies Phison's PS3110-S10 controller and Toshiba's MLC NAND Flash, and protection measures such as error-correction code, wear leveling management and data encryption are also adopted. Its operating voltage is 5V (±10%) DC, while the temperature limit range are −40°C∼+85°C for storage and 0° ∼ +70° for operation, respectively. The total data written is 257TB, approximately 3000∼5000 P/E cycles. An open-source Iometer based SSD test system software is specifically designed to realize the function of automatic parameter monitoring, including the voltage and current at the SATA interface, the average & real-time read/write speed and response time, as well as the amount of the written data. It can not only inspect and record the disk capacity periodically, but also adjust the test strategy (the read/write proportion, the data packet size, and the assess patterns), and control the power supply voltage. The testing system chart of SEE tests or thermal tests is shown in Fig. 2.

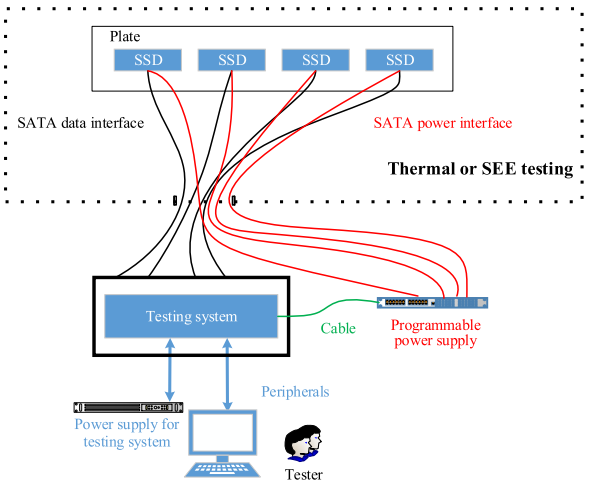

FIGURE 2. Testing system chart of SEE tests or thermal tests.

A. DATA SIMULATION

This commercial SSD is shown as an example to illustrate the procedure that how to predict reliability and RUL when read/write speed and current are used as precursor parameters. Hard failure data are generated based on similar components' SEE results of COTS A3PE3000L type FPGA in space application. Samples 1#∼4# are tested under three

different ion beams, and the ion characteristics and SEL cross sections are listed in Table 2. On the other hand, according to the previous constant stress ADT data of the military-grade SSDs, we simulate soft failure data with the model parameters presented in Table 3. Every four samples are randomly selected from the total twelve products (5#∼16#) to carry out thermal ADT under each accelerated stress levels with 80°C, 90°C and 110°C. Fig. 3 shows the simulated soft failure data, and we assume the failure threshold at practical operating temperature (40°C) is 125mA referencing to the NAND flash memory manual. It is apparent from the figure that the degradation of the random write current is nonlinear and physically dependent on the system aging, then the power law function with stress variances is justified.

TABLE 2. Ion beams and SEL cross sections of controller vs. Ion LET.

No.	Ion species	Energy /MeV	LET /(MeVcm^2/mg)	Range (Si)/ μm	Angle /(°)	SEL cross section(cm^2)			
						1	2	3	4
1	$^{35}Cl^{11}_{+}$	175	12.6	51.1	90	0.00 32	0.00 32+	0.00 32+	0.00 28
2	$^{74}Ge^{1}_{1,20+}$	235	36.8	33.4	90	0.02 58+	0.02 44	0.02 58	0.02 06
3	$^{127}I^{15,}_{25+}$	295	66.0	30.8	90	0.02 86	0.05 16	0.03 81	0.04 33

Note: "+" denote the truncated data

TABLE 3. Estimated model parameters and true values of the degradation model.

Parameters	a	b	σ	m	μ_c	σ_c	d	α	σ_B
True value	-	-	-	-	0.2	0.08	85	4.5	0.5
Estimation	-9.2397	1.4952	0.1800	5.5542	0.2221	0.1009	90.1252	4.5618	0.4226

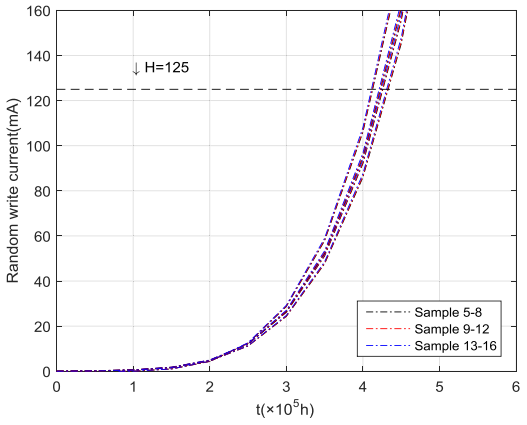

FIGURE 3. Degradation measurements of random write current data.

B. RELIABILITY ASSESSMENT

Obviously, some cross sections results are censored in Table 2. For curve fitting method, we usually adopt the average value at each LET for simplicity, and expect to find the best fitting curve. In this case, if we use the traditional curve fitting method, not only some censored information are ignored, but also unreasonable negative values are inevitable when LET is small. Thus, the proposed Weibull regression method can effectively avoid these drawbacks. By the estimation procedure in section IV-A, the hard failure parameter results are presented in Table 3. Then the conventional optimal curve fitting and the Weibull regression analysis results for censored failure data are compared respectively in Fig. 4.

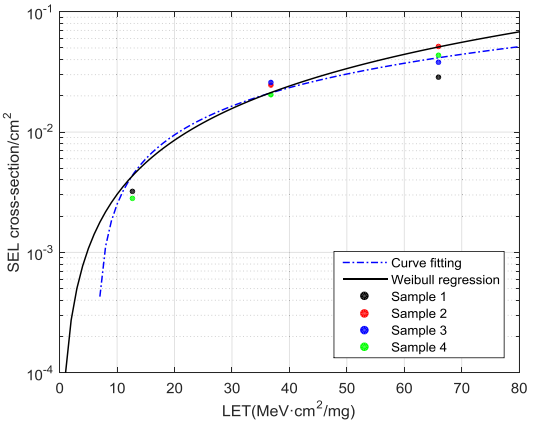

FIGURE 4. SEL cross-section of the controller vs ion LET.

Take the environment data of Tiangong-1 space module for example, the flux versus LET histogram within a solar maximum window at 350km orbital altitude is presented in Fig. 5. The shielding material is 5mm aluminum. LET spectra of galactic cosmic radiation (GCR) and solar proton events (SPEs) can be easily integrated. Then the hard failure reliability curves under varying LETs are illustrated in Fig. 6.

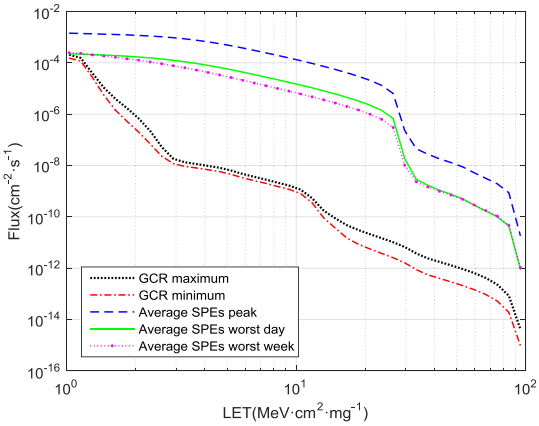

FIGURE 5. Average flux versus LET histogram of Tiangong-1 orbit (350km, 5mm shielding aluminum).

The degradation estimation results are also provided in Table 3. From this data, we can see that all the parameters' true and estimated values are approximately equal. Moreover, the true and estimated reliability curves in Fig. 7 for soft failures are very close to each other, further demonstrating the effectiveness of the proposed estimation method.

Failure probabilities under the competing risk model as well as hard and soft failures are shown in Fig. 8. Thus, we conclude that SEL is the dominant failure mechanism, and random write current degradation failure mode

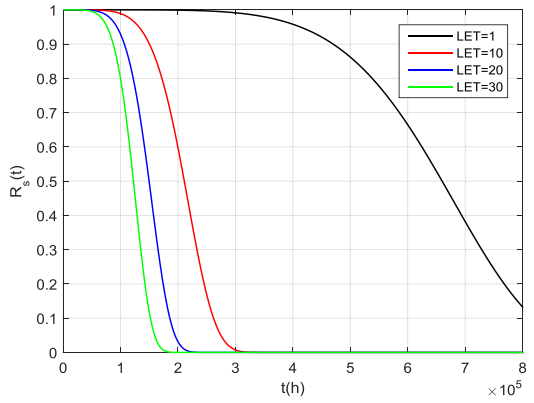

FIGURE 6. Reliability curves with hard failures under different LETs.

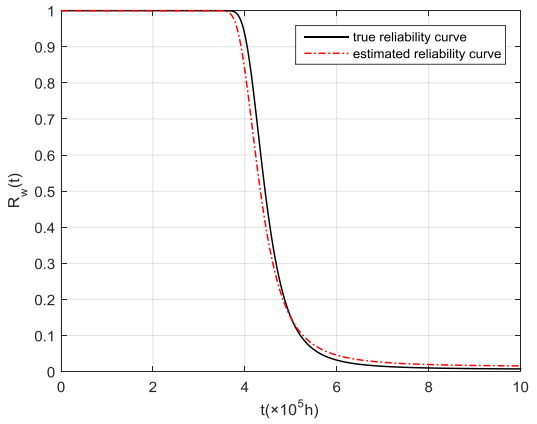

FIGURE 7. Reliability curves with soft failures under normal operating temperature (40°C).

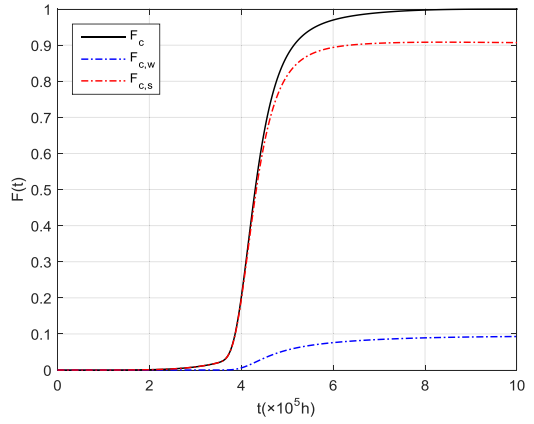

FIGURE 8. Estimate of cdf $F_c(t)$ under the competing risk model and of failure probabilities $F_{c,s}(t)$ and $F_{c,w}(t)$.

has little effect during the first 400000h. The asymptotic values of failure functions $F_{c,s}(t)$ and $F_{c,w}(t)$ are 0.9053 and 0.0947 respectively, which means random write current degradation accounts for approximately 9.47% of the whole failures.

To demonstrate the feasibility of the proposed method in RUL estimation, reliability curves with competing risk model under normal thermal stress and each LET levels are shown

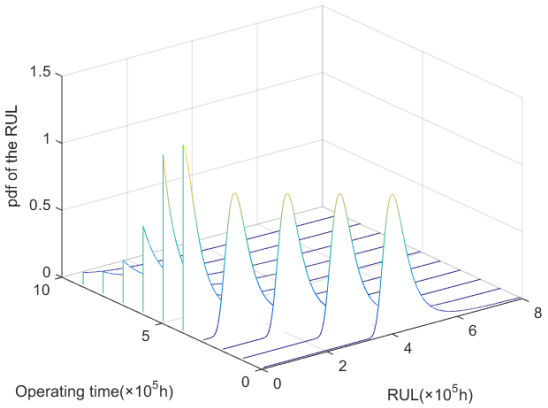

FIGURE 9. Reliability curves with competing risk model under normal thermal stress (40°C) and typical LET.

in Fig. 9, demonstrating the necessity of taking the nonlinear degradation process into consideration.

C. SENSITIVITY ANALYSIS

To investigate the effect of competing risk model parameters and provide the guidance to design accelerated test plan, sensitivity analyses of $R_c(t)$ on LET, S, H are presented in Fig. 9-11 respectively.

From Fig. 10, we observe that LETs have a remarkable effect on $R_c(t)$. Following the addition of LET, a significant decrease in the reliability under the competing risk model is recorded, indicating that ions with higher LETs are more likely to cause SSD breakdown. The result may be explained by the fact that as LET represents charged particles' direct ionization capacity in certain materials, the SSD may experience severer effect and have higher possibility to fail when the ions have higher LETs. Actually the plasma track caused by the radiation of high-energy particles can trigger the charge to flow within the track, and then catastrophic large current might continuously heat the chip until the SSD fails. While in Fig. 11, competing risk reliability is not obviously sensitive to the temperature S. When S increases from 20°C to 60°C, $R_c(t)$ slightly decreases. This result further supports the idea

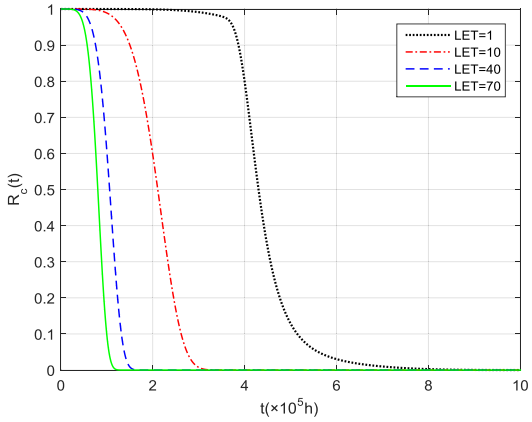

FIGURE 10. Sensitivity analysis of competing risk reliability on LETs.

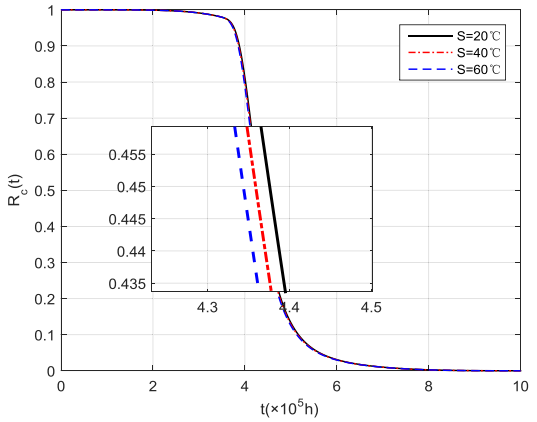

FIGURE 11. Sensitivity analysis of competing risk reliability on thermal stress levels.

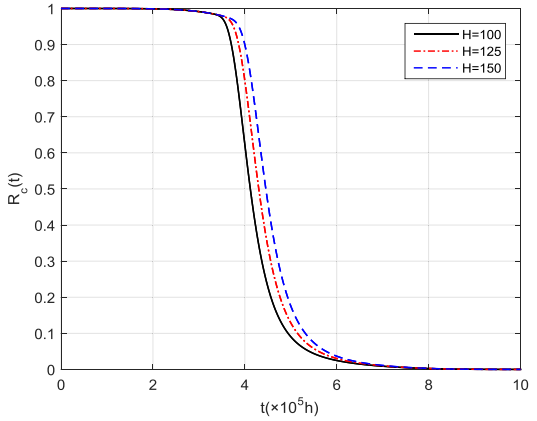

FIGURE 12. Sensitivity analysis of competing risk reliability on degradation failure threshold levels.

that high temperature intensifies the thermal motion energy of electrons, and then it accelerates the degradation and destruction process of the tunnel oxide, leading to an increasing moving read reference, raw bit error rate and defects per million. As shown in Fig. 12, the reliability under competing risk model is susceptible to the soft failure threshold, and the SSD performance is better for a higher failure threshold. In most cases, hard failure modes are obvious and easy to recognize, hence they are often acceptable for both users and manufacturers. However, there is usually a gap between their criteria to report a soft failure. For example, an SSD failure reported by its user might still in the operatable state based on the manufacturer's criterion. On the other hand, a failure defined by the manufacturer may be still satisfactory by its own user. In addition, the user satisfaction level might be different from one to another. Therefore, soft failure threshold uncertainty should be taken into consideration concerning reliablity modeling.

VI. CONCLUSION

In this paper, a new reliability analysis method is proposed to solve the competing risk modeling problem and demonstrate the rationality of using commercial NAND-based SSDs in the space field. On one hand, the SSD structure, function and principle analysis are presented. On the other hand, the SSD space environment effects, including platform stresses, operating stresses and space environment stresses during its on-orbit stage are analyzed comprehensively, and results indicate that ionizing radiation and temperature are dominant sensitive stresses that deserve extra attention. The controller's hard failure is primarily attributed to SEL, and high temperature causes the phenomenon of NAND Flash random write current degradation. The hard failure model is built based on the invariance principle of total environmental particles' energy. The inverse power law-Weibull model is used to characterize hard failures, while a nonlinear Wiener-process-based ADT model with temporal variability and unit-to-unit variability is developed for soft failures. Then the reliability and RUL functions considering competing failures are eventually obtained. Furthermore, the Weibull regression analysis method for censored data and the MLE method for degradation data are developed to estimate model parameters respectively. At last, the effectiveness of the newly proposed reliability model is illustrated by a simulated case study with sensitivity analysis. The numerical example shows that the proposed method can efficiently verify whether it is feasible to apply commercial NAND-based SSDs in the space field.

For further investigation of this work, SSD failure analysis based on practical experiments should be highlighted to help design changes or provide corrective actions, and measurement errors and model uncertainty can be studied to implement more accurate estimation and prognostic. Moreover, dynamic reliability analysis considering dependent failures can be investigated to further improve the developed model.

REFERENCES

[1] Y. Cai, S. Ghose, E. F. Haratsch, Y. Luo, and O. Mutlu, "Error characterization, mitigation, and recovery in flash-memory-based solid-state drives," *Proc. IEEE*, vol. 105, no. 9, pp. 1666–1704, Sep. 2017.

[2] G. S. Choi and B.-W. On, "Study of the performance impact of a cache buffer in solid-state disks," *Microprocess. Microsyst.*, vol. 35, no. 3, pp. 359–369, May 2011.

[3] M. Fabiano and G. Furano, "NAND flash storage technology for mission-critical space applications," *IEEE Aerosp. Electron. Syst. Mag.*, vol. 28, no. 9, pp. 30–36, Sep. 2013.

[4] B. Schroeder, A. Merchant, and R. Lagisetty, "Reliability of NAND-based SSDs: What field studies tell Us," *Proc. IEEE*, vol. 105, no. 9, pp. 1751–1769, Sep. 2017.

[5] A. Durier, A. Bensoussan, M. Zerarka, C. Ghfiri, A. Boyer, and H. Frémont, "A methodologic project to characterize and model COTS component reliability," *Microelectron. Rel.*, vol. 55, nos. 9–10, pp. 2097–2102, Aug./Sep. 2015.

[6] *Solid-State Drive (SSD) Endurance Workloads*, Standard JESD219A, 2012.

[7] *Solid-State Drive (SSD) Requirements and Endurance Test Method*, Standard JESD218B.01, 2016.

[8] N. R. Mielke, R. Frickey, I. Kalastirsky, M. Quan, D. Ustinov, and V. J. Vasudevan, "Reliability of solid-state drives based on NAND flash memory," *Proc. IEEE*, vol. 105, no. 9, pp. 1725–1750, Sep. 2017.

[9] C. M. Compagnoni, A. Goda, A. S. Spinelli, P. Feeley, A. L. Lacaita, and A. Visconti, "Reviewing the evolution of the NAND flash technology," *Proc. IEEE*, vol. 105, no. 9, pp. 1609–1633, Sep. 2017.

[10] S. Boyd, A. Horvath, and D. Dornfeld, "Life-cycle assessment of NAND Flash memory," *IEEE Trans. Semicond. Manuf.*, vol. 24, no. 1, pp. 117–124, Feb. 2011.

[11] K. Rafiee, Q. Feng, and D. W. Coit, "Reliability assessment of competing risks with generalized mixed shock models," *Rel. Eng. Syst. Saf.*, vol. 159, pp. 1–11, Mar. 2017.
[12] S. Hao, J. Yang, X. Ma, and Y. Zhao, "Reliability modeling for mutually dependent competing failure processes due to degradation and random shocks," *Appl. Math. Model. Appl. Math. Model.*, vol. 51, pp. 232–249, Nov. 2017.
[13] H. Che, S. Zeng, J. Guo, and Y. Wang, "Reliability modeling for dependent competing failure processes with mutually dependent degradation process and shock process," *Rel. Eng. Syst. Saf.*, vol. 180, pp. 168–178, Dec. 2018.
[14] Q. Qiu and L. Cui, "Reliability evaluation based on a dependent two-stage failure process with competing failures," *Appl. Math. Model.*, vol. 64, pp. 699–712, Dec. 2018.
[15] S. Hao and J. Yang, "Reliability analysis for dependent competing failure processes with changing degradation rate and hard failure threshold levels," *Comput. Ind. Eng.*, vol. 118, pp. 340–351, Apr. 2018.
[16] F. Haghighi and S. J. Bae, "Reliability estimation from linear degradation and failure time data with competing risks under a step-stress accelerated degradation test," *IEEE Trans. Rel.*, vol. 64, no. 3, pp. 960–971, Sep. 2015.
[17] M. Fan, Z. Zeng, E. Zio, and R. Kang, "Modeling dependent competing failure processes with degradation-shock dependence," *Rel. Eng. Syst. Saf.*, vol. 165, pp. 422–430, Sep. 2017.
[18] M. Fan, Z. Zeng, E. Zio, R. Kang, and Y. Chen, "A stochastic hybrid systems based framework for modeling dependent failure processes," *PLoS ONE*, vol. 12, no. 2, Feb. 2017, Art. no. e0172680.
[19] M. Fan, Z. Zeng, E. Zio, R. Kang, and Y. Chen, "A sequential Bayesian approach for remaining useful life prediction of dependent competing failure processes," *IEEE Trans. Rel.*, to be published. doi: 10.1109/TR.2018.2874459.
[20] X. S. Si, "An adaptive prognostic approach via nonlinear degradation modeling: Application to battery data," *IEEE Trans. Ind. Electron.*, vol. 62, no. 8, pp. 5082–5096, Aug. 2015.
[21] P. Li, C. Li, and W. Dang, "Accelerated reliability demonstration testing design based on reliability allocation of environmental stresses," *Qual. Rel. Eng. Int.*, vol. 33, no. 7, pp. 1425–1435, Nov. 2017.
[22] X.-S. Si, W. Wang, C.-H. Hu, D.-H. Zhou, and M. G. Pecht, "Remaining useful life estimation based on a nonlinear diffusion degradation process," *IEEE Trans. Rel.*, vol. 61, no. 1, pp. 50–67, Mar. 2012.
[23] Z. Zhang, X. Si, C. Hu, and Y. Lei, "Degradation data analysis and remaining useful life estimation: A review on Wiener-process-based methods," *Eur. J. Oper. Res.*, vol. 271, no. 3, pp. 775–796, Dec. 2018.
[24] P. Li, K. Liu, W. Dang, and T. Zou, "Reliability assessment of NAND SSD based on acceleration degradation test," in *Proc. IEEE IEEM*, Singapore, Dec. 2017, pp. 1945–1949.
[25] M. V. O'Bryan *et al.*, "Compendium of current single event effects for candidate spacecraft electronics for NASA," in *Proc. IEEE REDW*, Boston, MA, USA, Jul. 2015, pp. 45–53.
[26] S. C. Davis, R. Koga, and J. S. George, "Proton and heavy ion testing of the microsemi Igloo2 FPGA," in *Proc. IEEE REDW*, New Orleans, LA, USA, Jul. 2017, pp. 168–173.
[27] R. Sayyad and S. Redkar, "Failure analysis and reliability study of NAND Flash-based solid state drives," *Ind. J. Elect. Eng. Comput. Sci.*, vol. 2, no. 2, pp. 315–327, May 2016.
[28] D. Bocchetti, M. Giorgio, M. Guida, and G. Pulcini, "A competing risk model for the reliability of cylinder liners in marine Diesel engines," *Rel. Eng. Syst. Saf.*, vol. 94, no. 8, pp. 1299–1307, Aug. 2009.
[29] J. Qi, Z. Zhou, C. Niu, C. Wang, and J. Wu, "Reliability modeling for humidity sensors subject to multiple dependent competing failure processes with self-recovery," *Sensors*, vol. 18, no. 8, p. 2714, Aug. 2018.
[30] J. Luo *et al.*, "Influence of heavy ion flux on single event effect testing in memory devices," *Nucl. Instrum. Methods Phys. Res. B, Beam Interact. Mater. At.*, vol. 406, pp. 431–436, Sep. 2017.
[31] F. Wrobel, A. D. Touboul, V. Pouget, L. Dilillo, J. Boch, and F. Saigné, "A calculation method to estimate single event upset cross section," *Microelectron. Rel.*, vol. 76, pp. 644–649, Sep. 2017.
[32] S. Hao, J. Yang, and C. Berenguer, "Nonlinear step-stress accelerated degradation modelling considering three sources of variability," *Rel. Eng. Syst. Saf.*, vol. 172, pp. 207–215, Apr. 2018.
[33] Y. Wang, Y. Peng, Y. Zi, X. Jin, and K. L. Tsui, "A two-stage data-driven-based prognostic approach for bearing degradation problem," *IEEE Trans. Ind. Informat.*, vol. 12, no. 3, pp. 924–932, Jun. 2016.
[34] N. Balakrishnan and P. S. Chan, "Order statistics from extreme value distribution, I: Tables of means, variances and covariances," *Commun. Statist.-Simul. Comput.*, vol. 21, no. 4, pp. 1199–1217, Jun. 1992.
[35] S. Tang, X. Guo, and Z. Zhou, "Mis-specification analysis of linear Wiener process–based degradation models for the remaining useful life estimation," *Proc. Inst. Mech. Eng., O, J. Risk Rel.*, vol. 228, no. 5, pp. 478–487, Oct. 2014.

PENG LI received the B.S. degree in control engineering from Central South University, Changsha, in 2013, and the M.S. degree in reliability engineering from Beihang University, Beijing, China, in 2016. He is currently pursuing the Ph.D. degree in computer application with the University of Chinese Academy of Sciences, Beijing.

Since 2016, he has been a Reliability Engineer with the Technology and Engineering Center for Space Utilization, Chinese Academy of Sciences, Beijing. His research interests include reliability modeling and assessment, environmental test design and analysis, and space components' assurance.

WEI DANG received the B.S. degree in quality and reliability engineering from Beihang University, Beijing, China, in 2004, and the M.S. degree in flight vehicle design from the University of the Chinese Academy of Sciences, Beijing, in 2007.

He is currently an Associate Professor and the Director of the Reliability Assurance Center, Technology and Engineering Center for Space Utilization, Chinese Academy of Sciences. His research interests include reliability systems' engineering, commercial off-the-shelf components, big data, and AI.

TAICHUN QIN received the Ph.D. degree in systems engineering from Beihang University, Beijing, China, in 2018.

He is currently an Engineer with the Beijing Key Laboratory of Environment and Reliability Test Technology for Aerospace Mechanical and Electrical Products, Beijing Institute of Spacecraft Environment Engineering. His research interests include battery management systems, prognostics and health management, and reliability test and analysis.

ZEMING ZHANG received the master's degree in optical engineering from the Beijing Institute of Technology, Beijing, China, in 2002.

He is currently an Associate Professor of aerospace component quality assurance with the Technology and Engineering Center for Space Utilization, Chinese Academy of Sciences. His research interest includes commercial off-the-shelf component application in the space field.

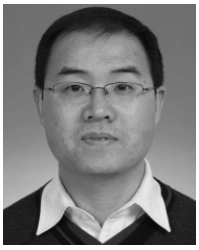

CONGMIN LV received the B.S. degree in thermal engineering and power machinery from the Wuhan University of Technology, Wuhan, in 1995, the M.S. degree in power machinery and engineering from Jilin University, Changchun, in 1998, and the Ph.D. degree in space physics from the University of Chinese Academy of Sciences, Beijing, China, in 2004.

He is currently a Professor with the Technology and Engineering Center for Space Utilization, Chinese Academy of Sciences. He is also the Vice Chief Designer for the space application system of the Manned Space Flight Project. His research interests include space physics, mirogravity, and reliability engineering.